Supplement of Atmos. Chem. Phys., 24, 5625–5636, 2024
https://doi.org/10.5194/acp-24-5625-2024-supplement

Atmospheric Chemistry and Physics
Open Access
EGU

Supplement of

Suppressed atmospheric chemical aging of cooking organic aerosol particles in wintertime conditions

Wenli Liu et al.

Correspondence to: Mikinori Kuwata (kuwata@pku.edu.cn)

Section S1. ME-2 analysis

ME-2 analysis was used to estimate mass fractions of 'fresh COA' and 'oxidized COA' in particles for each experimental condition. 10~15 sets of mass spectra with the range of m/z = 41 to 210, excluding 44, at each position were employed for the analysis. The mass spectra of COA particles prior to ozone exposure were employed as seed profiles for the analysis. The mass spectra for the high ozone exposure (7 ppm, 60 s of exposure time) at 25 °C were analyzed together with each experimental dataset to constrain the profiles for reaction products.

The number of factors was changed for the range of 2 to 4 to evaluate the appropriate factor number using the data for Exp. #1. The resulting ratio of the sum of squared residuals weighted (Q) by their uncertainties to the degree of freedom of model solution calculated based on the size of the data matrix and the number of factors ($Qexp$) is one important metric to judge the appropriateness of the solution. $Q/Qexp$ values decreased from 1.9 to 1.47 as factor numbers increased from 2 to 3. For the 4-factor analysis, it kept decreasing but was not that significant (1.29).

In the case of 2-factor analysis, dominated ions in the mass spectra (Fig. S5) were almost the same for the two factors. However, the factor analysis successfully resolved marker ions for 'fresh COA' (e.g., m/z = 191 and 202) and certain reaction products (e.g., m/z = 155). Mass spectra for the factors in the 3-factor analysis are shown in Fig. S13. Factor 1 exhibited a very high correlation (R^2>0.999) with the seed profile, which was treated as the 'fresh COA'. Peak at m/z = 155, the marker ion for 'oxidized COA', was significant in factor 2. Changes in mass fraction at each data point (Fig. S14) reconfirmed that factor 1 and factor 2 corresponded to 'fresh COA' and 'oxidized COA'. The mass spectrum of factor 3 showed higher similarity with factor 2. The contribution of factor 3 was negligible except for the high ozone exposure period. We speculate that the factor might correspond to reaction products that are not produced by the initial ozonolysis. The existence of factor 3 does not influence the estimation of k_2, as we employed the loss of 'fresh COA' for calculating the parameter. No factor in the 4-factor analysis corresponded to the 'fresh COA' (Fig. S15). As a result, two-factor solutions were employed in the present research.(Budisulistiorini et al., 2021; Liu et al., 2023)

The degree of freedom (a value) was also changed from 0.0 to 1.0 with the interval of 0.1 for optimizing the analysis. Figure S16 shows the corresponding Q/Q_{exp} values for Exp. #1, 7, 9, 10, 20 and 21. The Q/Q_{exp} values decreased significantly when the a value increased from 0 to 0.1. The value slightly decreased from 0.1 to 0.2. No apparent change in the Q/Q_{exp} values was observed for higher a value. The mass spectra of factor 1 for the above-mentioned experimental runs exhibited a high correlation (R^2 > 0.999) with the seed profile among all the a value tests. We set the a value to be 0.2 in the present study, based on the above-mentioned conditions.

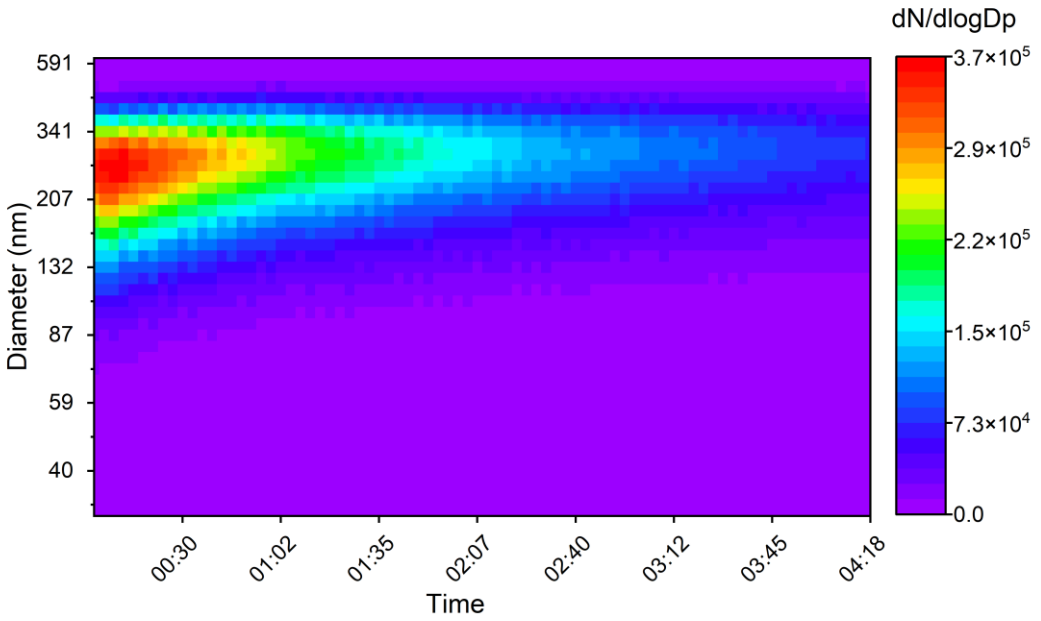

Figure S1. Normalized size distributions of lard COA particles in the tank. Particle injection was stopped at time zero.

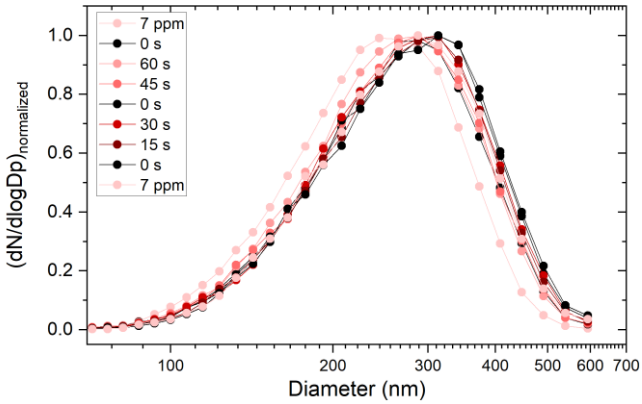

Figure S2. Normalized size distributions of canola oil COA particles during Exp. #1. Time scales in legend indicate the reaction time for COA particles with ozone under ozone concentration of 450 ppb. Reaction time for 7 ppm experiments was 60 s.

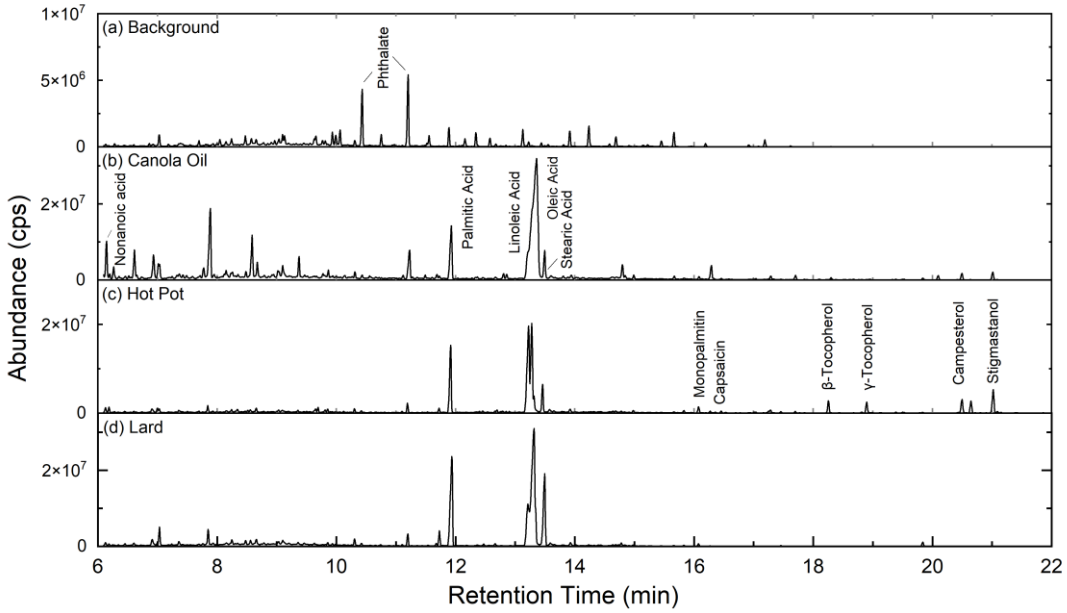

Figure S3. Gas chromatograms of (a) background, (b) canola oil, (c) hot pot and (d) lard COA particles.

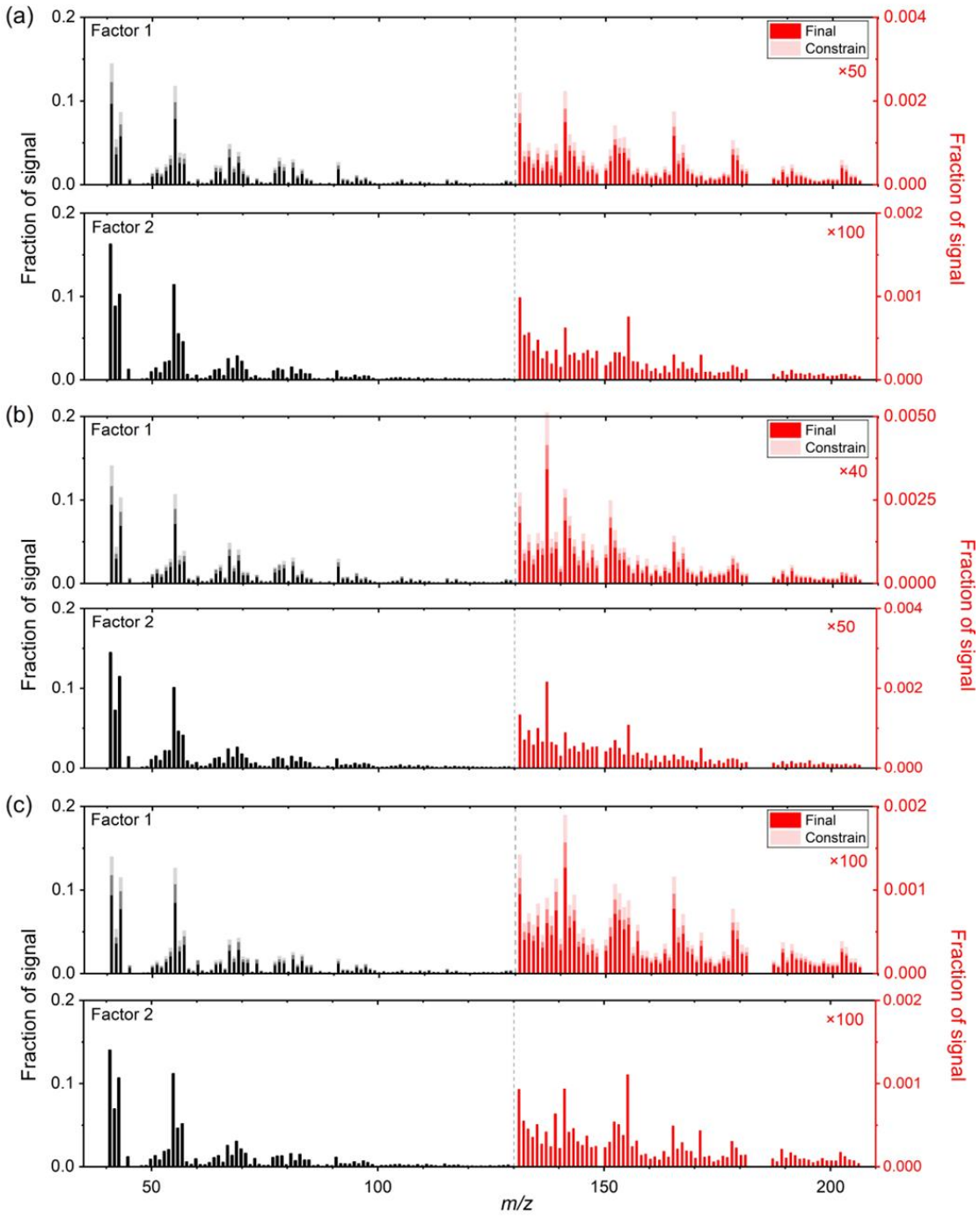

Figure S4. Mass spectra of factor 1 and factor 2 for (a) canola oil Exp. #1, (b) hot pot Exp. #9, (c) lard Exp. #20 COA particles. Dark color bars indicate the resulting profile from the factor analysis, while the light color bars correspond to the constrained ranges for factor 1 during the analysis. The signal fractions of *m*/*z* of 130~210 are enhanced by different times as noted in the graph.

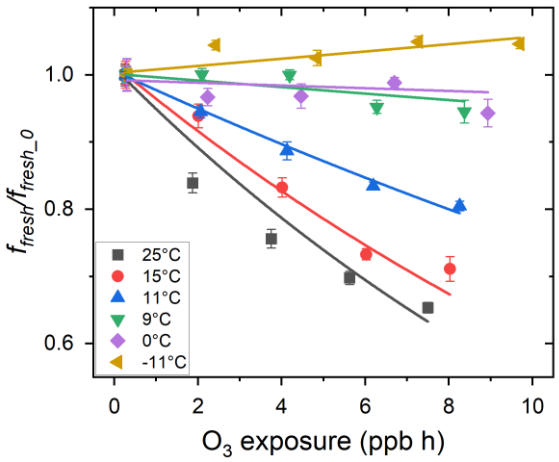

Figure S5. Changes in mass fractions of 'fresh COA' (f_{fresh}) for lard experiments induced by ozone exposure. The value of f_{fresh} prior to ozone exposure was denoted as $f_{fresh\text{-}0}$. The data were colored by temperature of the flow tube. The positive slope for fitting line for -11°C experiment was not employed for the calculation of k_2.

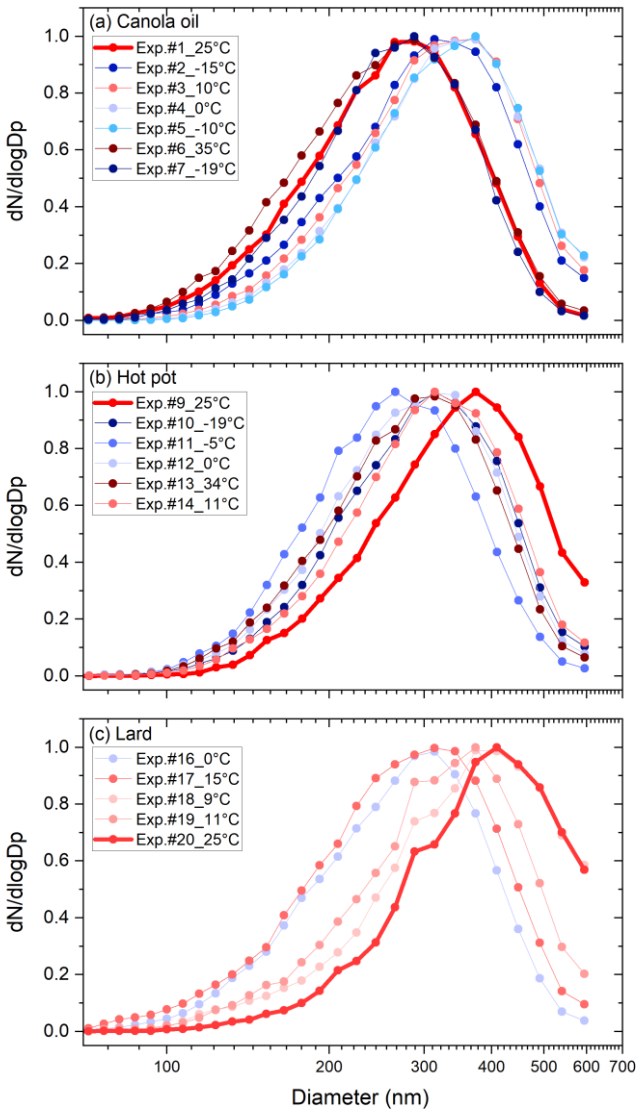

Figure S6. Normalized size distributions of laboratory generated (a) canola oil, (b) hot pot, (c) lard COA particles following coagulation. Size distributions of particles were recorded every 3 minutes in 60 bins for the diameter range of 10-600 nm (only the range of 70-600 nm was shown). Data for experiments at room temperature were shown in bold lines.

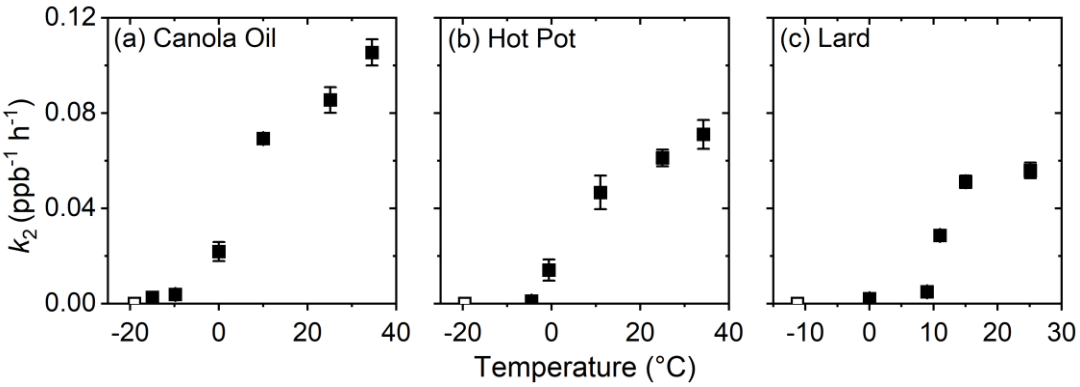

Figure S7. Values of k_2 for (a) canola oil, (b) hot pot, and (c) lard COA particles at various temperatures. The values of k_2 for Exp. #7, 10 and 21 were unmeasurably small for our experimental setup. Thus, they were shown in open symbols at the bottom.

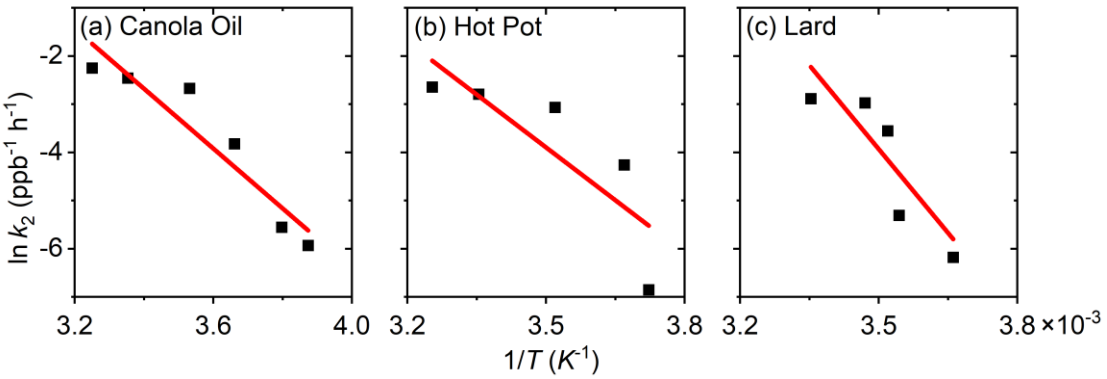

77

78 **Figure S8**. k_2-T relationship of (a) canola oil, (b) hot pot, and (c) lard COA particles fit by the
79 Arrhenius equation $lnk_2 = lnA - \frac{E_a}{RT}$.

80

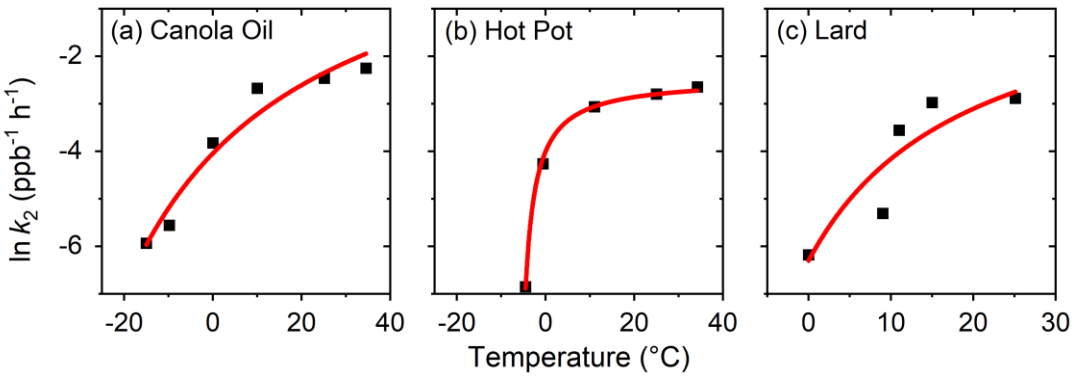

81

82 **Figure S9**. k_2-T relationship of (a) canola oil, (b) hot pot, and (c) lard COA particles fit by the
83 Vogel–Fulcher–Tammann (VFT) equation $\ln k_2 = \alpha_1 + \frac{\alpha_2}{T+\alpha_3}$.

84

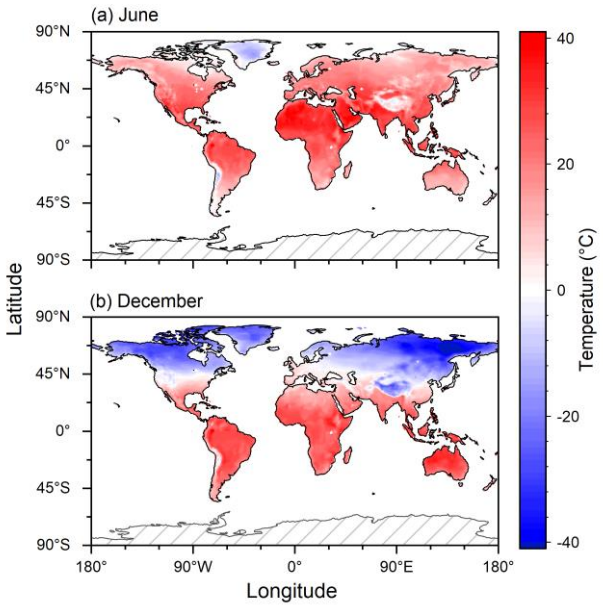

Figure S10. Monthly mean surface air temperatures during (a) June and (b) December of 2021. Data were obtained from the website of the Physical Sciences Laboratory of NOAA (https://psl.noaa.gov/mddb2/makePlot.html? variableID=1603).

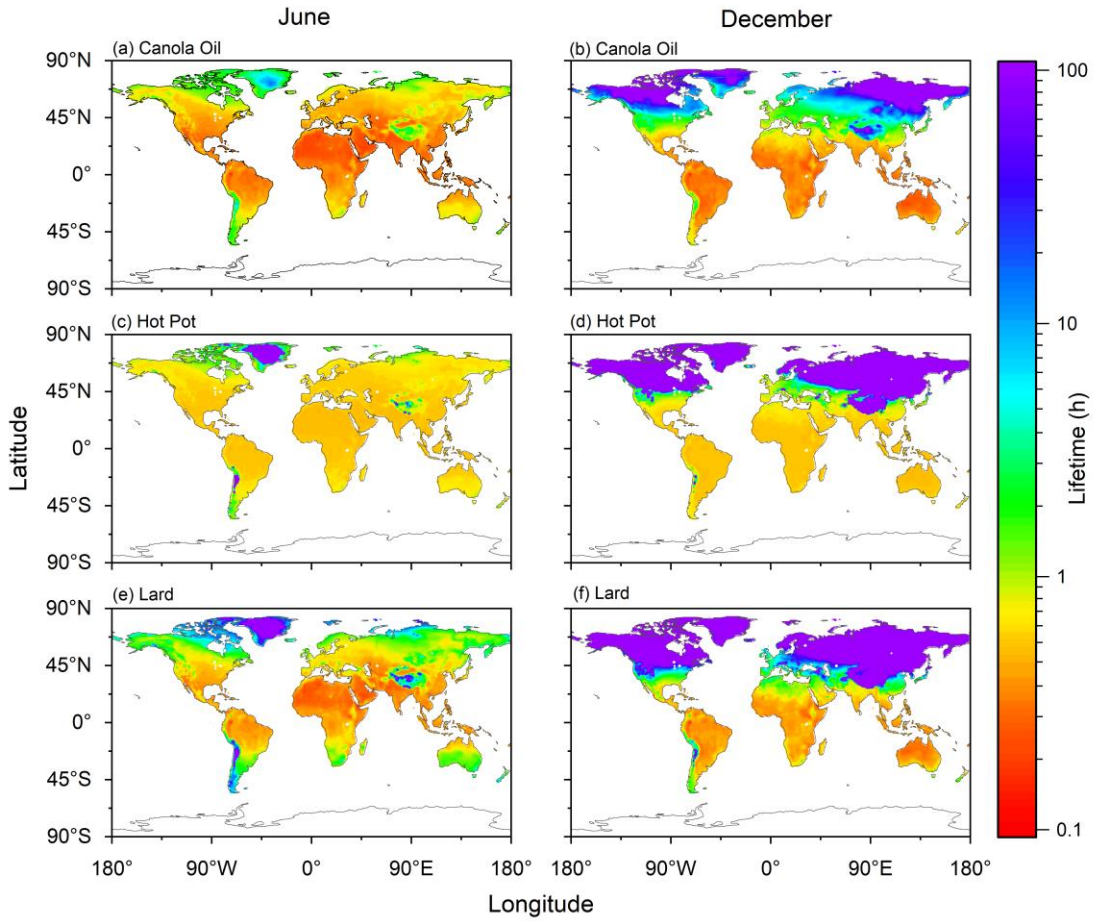

Figure S11. The estimated atmospheric chemical lifetime of cooking organic aerosols during (a,c,e) June and (b,d,f) December. Relationships between reaction rate constants k_2 and temperature were from the parameterization of (a,b) canola oil; (c,d) pot hot and (e,f) lard experiment results. Ozone concentration was assumed as 30 ppb.

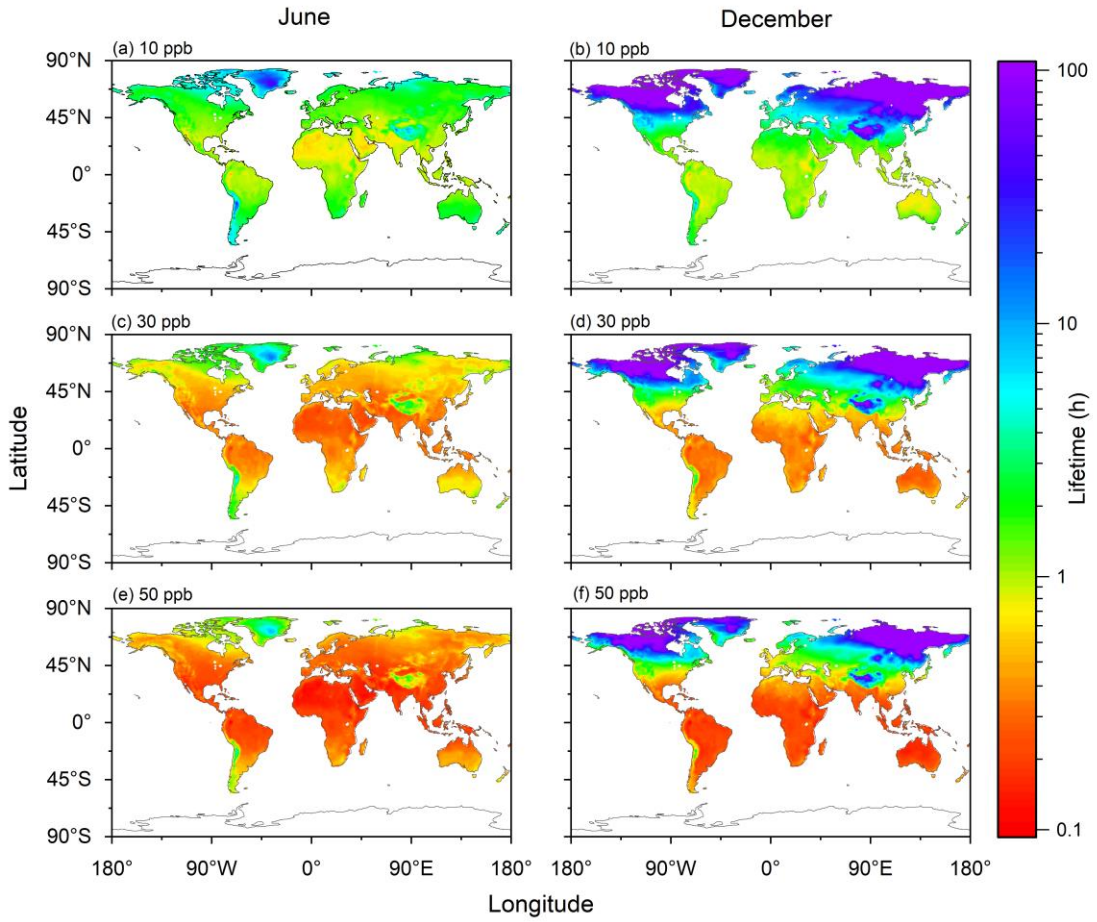

Figure S12. The estimated atmospheric chemical lifetime of cooking organic aerosols during (a,c,e) June and (b,d,f) December. The k_2-T relationship for the canola oil experiment results were employed. Ozone concentrations were assumed to be (a,b) 10 ppb; (c,d) 30 ppb and (e,f) 50 ppb.

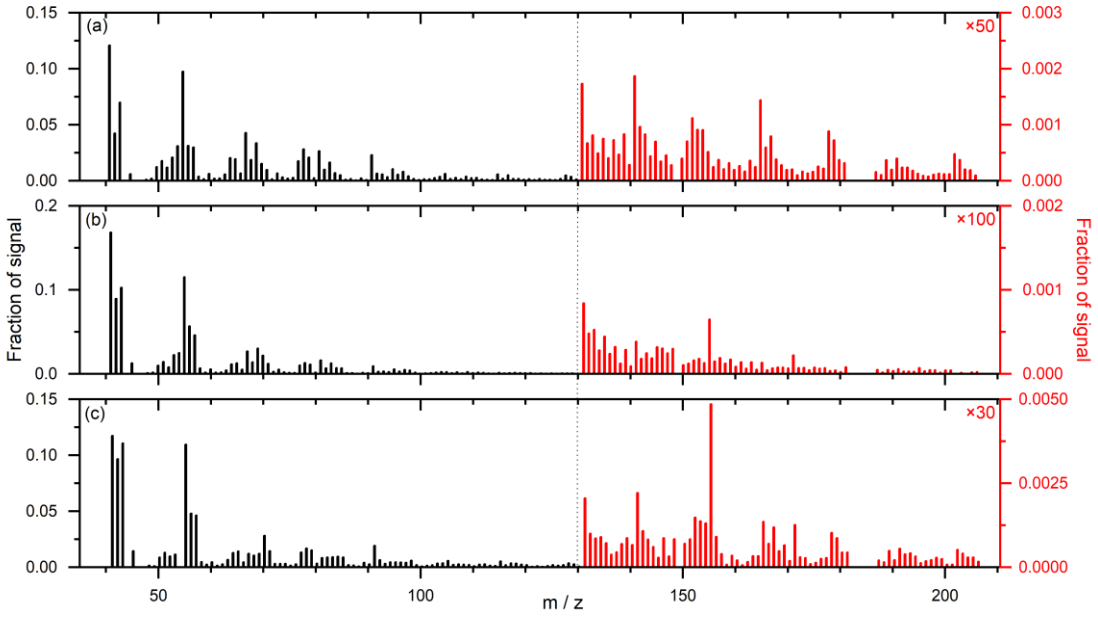

Figure S13. Mass spectra of (a) factor 1, (b) factor 2 and (c) factor 3 for the 3-factor analysis for canola oil Exp. #1. The signal fractions of *m*/*z* of 130~210 are enhanced by different times as noted on the graph.

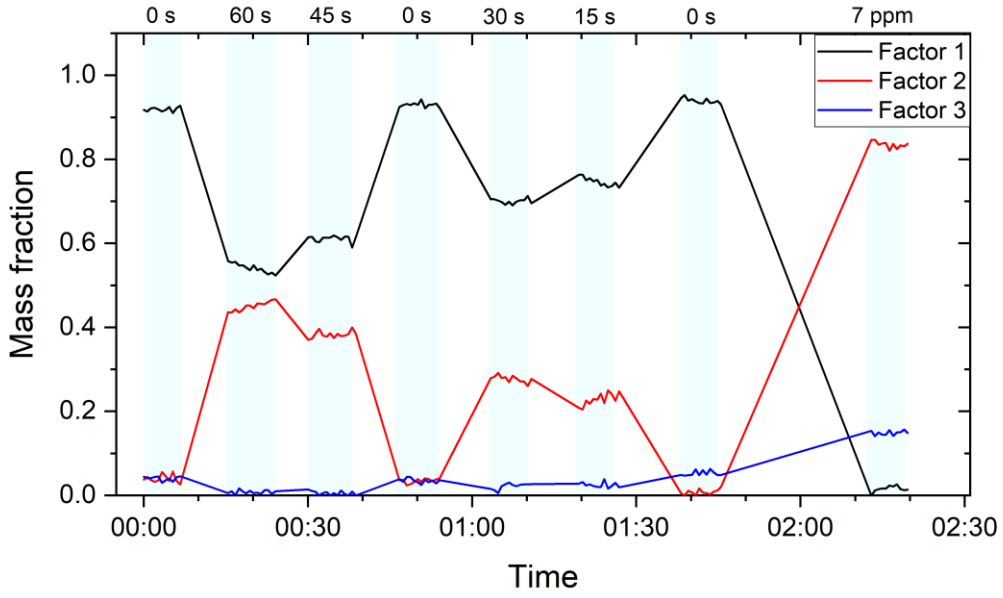

Figure S14. Time series plot for the contributions of three factors in the 3-factor analysis of canola oil Exp. #1. Values at the top indicate the reaction time for COA particles with ozone. Reaction time for 7 ppm experiments was 60 s.

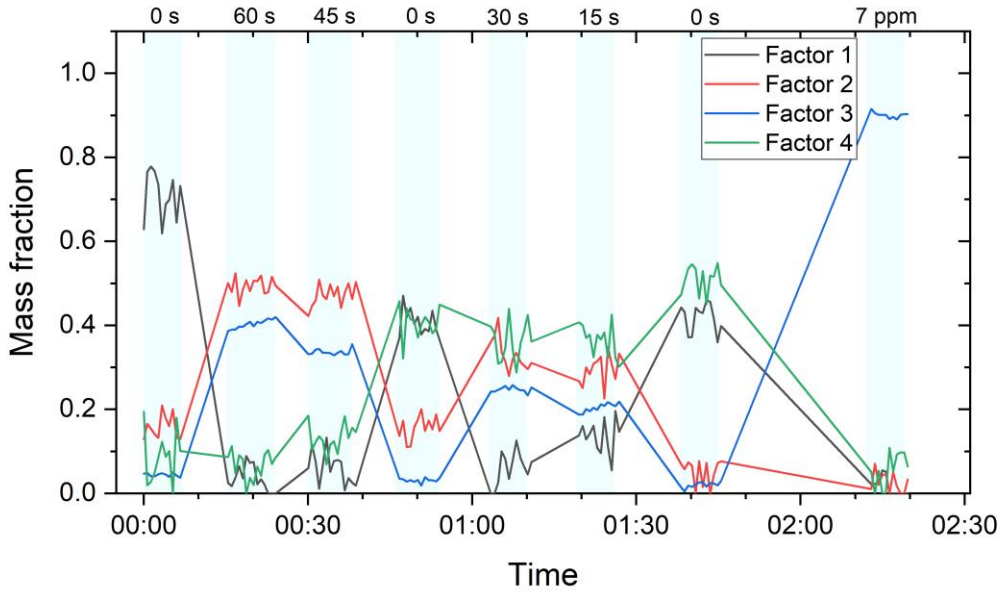

Figure S15. Time series plot for the contributions of the four factors in the 4-factor analysis of canola oil Exp. #1. Values at the top indicate the reaction time for COA particles with ozone. Reaction time for 7 ppm experiments was 60 s.

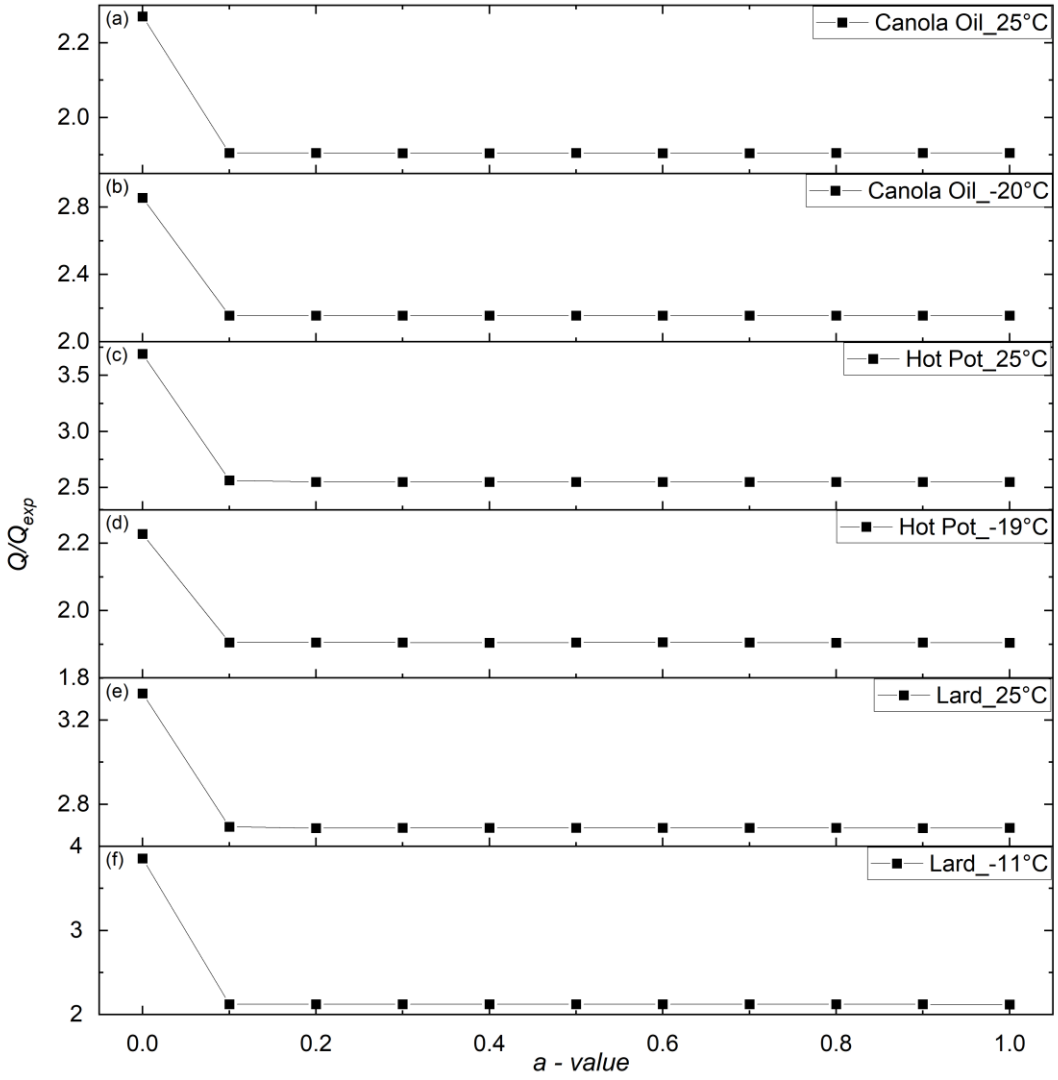

Figure S16. Dependence of Q/Q_{exp} values on a value for the ME-2 analyses of (a, b) canola oil (c, d) hot pot and (e,f) lard experiments at room and the lowest temperatures.

Table S1. Summary of the experiments for the present study.

Exp. #	COA type	*T* (°C)	Analysis
1	Canola Oil	25	ACSM and SEMS
2	Canola Oil	-15	ACSM and SEMS
3	Canola Oil	10	ACSM and SEMS
4	Canola Oil	0	ACSM and SEMS
5	Canola Oil	-10	ACSM and SEMS
6	Canola Oil	34.5	ACSM and SEMS
7	Canola Oil	-19	ACSM and SEMS
8	Canola Oil	25	SV-TAG and OPC
9	Hot Pot	25	ACSM and SEMS
10	Hot Pot	-19.5	ACSM and SEMS
11	Hot Pot	-4.5	ACSM and SEMS
12	Hot Pot	-0.5	ACSM and SEMS
13	Hot Pot	34	ACSM and SEMS
14	Hot Pot	11	ACSM and SEMS
15	Hot Pot	25	SV-TAG and OPC
16	Lard	0	ACSM and SEMS
17	Lard	15	ACSM and SEMS
18	Lard	9	ACSM and SEMS
19	Lard	11	ACSM and SEMS
20	Lard	25	ACSM and SEMS
21	Lard	-11	ACSM and SEMS
22	Lard	25	SV-TAG and OPC

Table S2. Standards used for SV-TAG in the present study.

Calibration standards in experiment		
Compound	Purity	Company
Oleic acid	99.8%	Shanghai Macklin Biochemical Co., Ltd
Linoleic acid	99%	Shanghai Macklin Biochemical Co., Ltd
Stearic acid	99%	Shanghai Aladdin Biochemical Technology Co., Ltd
Palmitic acid	99%	Shanghai Aladdin Biochemical Technology Co., Ltd

Table S3. Optimized parameters of Vogel–Fulcher–Tammann (VFT) equation fitting for three COA.

	α_1	α_2	α_3
Canola Oil	1.67	-340.6	59.6
Hot Pot	-2.46	-10.6	6.9
Lard	0	-111.4	17.9

Reference

Budisulistiorini, S. H., Chen, J., Itoh, M., and Kuwata, M.: Can online aerosol mass spectrometry analysis classify secondary organic aerosol (SOA) and oxidized primary organic aerosol (OPOA)? A case study of laboratory and field studies of Indonesian biomass burning, ACS Earth Space Chem., 5, 3511-3522, https://doi.org/10.1021/acsearthspacechem.1c00319, 2021.

Liu, W., Liao, K., Chen, Q., He, L., Liu, Y., and Kuwata, M.: Existence of crystalline ammonium sulfate nuclei affects chemical reactivity of oleic acid particles through heterogeneous nucleation, J. Geophys. Res.: Atmos., 128, e2023JD038675, https://doi.org/10.1029/2023JD038675, 2023.